

# UpJoint: Updating 3D-Printed Joints for Various Wood Species

Ren Sato  
g2125035@fun.ac.jp  
Future University Hakodate  
Japan

Maria Larsson  
ma.ka.larsson@gmail.com  
The University of Tokyo  
Japan  
Aalto University  
Finland

Hironori Yoshida  
hyoshida@hy-ma.com  
Future University Hakodate  
Japan  
Aalto University  
Finland

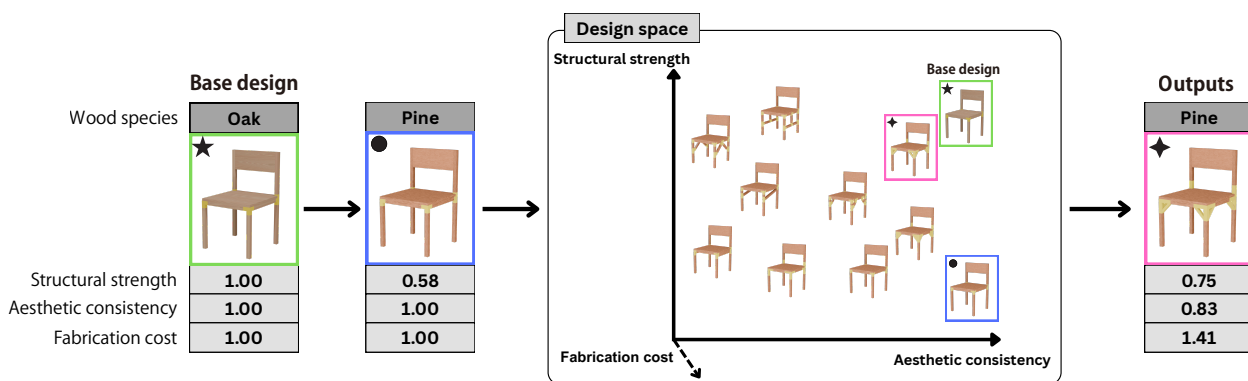


Figure 1: Based on the selected wood species, preferred load, and evaluation policy, UpJoint suggests design updates to a base chair that balance structural, aesthetic, and fabrication scores.

## Abstract

We present UpJoint, a computational system that adapts a base chair design to different wood species while balancing structural strength, aesthetic consistency, and fabrication cost. To support flexible adaptation without requiring changes to machining setups, we employ an assembly strategy based on wooden components connected by 3D-printed joints. The system introduces two core components: a design space for structural reinforcement and a model for evaluating aesthetic consistency. The design space was informed by a preliminary study and includes four update strategies, two of which involve inserting new structural members. Each strategy is parameterized to produce a broad set of viable design alternatives. While strength and fabrication cost are estimated from geometry and material data, aesthetic consistency is learned from human pairwise comparisons collected through a survey, and modeled using the Crowd-BT algorithm to infer a global preference ranking. We evaluated the system across four wood species and different optimization policies, highlighting distinct trade-offs between structure and appearance. We further validate our approach through physical joint testing and fabrication of a prototype.

## CCS Concepts

- Computing methodologies → Real-time simulation; • Human-centered computing → Interaction design.

## Keywords

design system, joinery, 3D-printing, additive manufacturing, wood, furniture, aesthetic consistency

## ACM Reference Format:

Ren Sato, Maria Larsson, and Hironori Yoshida. 2025. UpJoint: Updating 3D-Printed Joints for Various Wood Species. In *ACM Symposium on Computational Fabrication (SCF '25)*, November 20–21, 2025, Cambridge, MA, USA. ACM, New York, NY, USA, 13 pages. <https://doi.org/10.1145/3745778.3766648>

## 1 Introduction

With the recent rise in lumber prices, furniture manufacturers are increasingly turning to a broader range of wood species, particularly locally sourced varieties. However, furniture designs are typically tailored to the specific characteristics of a given species, taking into account both practical and aesthetic considerations. Wood species vary not only in appearance but also in mechanical properties such as hardness and density, which have a substantial impact on structural performance. For instance, oak is approximately five times stronger than balsa. Therefore, changing the wood species can undermine the base design.

Moreover, furniture designs must also consider manufacturing constraints, including logistics and material processing equipment. To enable design updates without necessitating changes to machining setups—such as jigs or fixture configurations—3D-printed connectors offer a flexible alternative for joining wooden components. This strategy reduces the effort required to switch between different wood species without reorganizing the production line. Ideally, a single furniture design would accommodate multiple wood species simply by updating the 3D-printed joints while maintaining the impression of the base design.



This work is licensed under a Creative Commons Attribution 4.0 International License.  
SCF '25, Cambridge, MA, USA  
© 2025 Copyright held by the owner/author(s).  
ACM ISBN 979-8-4007-2034-5/2025/11  
<https://doi.org/10.1145/3745778.3766648>

Prior work has leveraged the adaptability of 3D-printed connectors by automatically adjusting them to various angles and component shapes, and in some cases optimizing for strength and/or fabrication cost (material usage) [7, 19, 20, 26]. However, our setting introduces new challenges by involving a reference base design. First, **structural reinforcement** of the base design may be required when the substituted material has weaker mechanical properties. Second, **aesthetic consistency** becomes critical: the updated design should preserve the base design’s overall visual impression. Addressing these challenges is non-trivial, as reinforcement involves navigating a vast design space, and added members can significantly alter the look and feel of the piece. Thus, there is a need for methods that balance structural adaptation with aesthetic continuity.

To address these challenges, we introduce UpJOINT, a system that adapts a given furniture design to different wood species while balancing structural strength, aesthetic consistency, and fabrication cost. Specifically, we developed the system for a basic chair design composed of wooden components connected by 3D-printed joints. Given a new wood species, a load requirement, and a user-defined selection policy, UpJOINT suggests an updated design that balances the three objectives according to the policy.

The system contains two key components: 1) a design space for structural reinforcement, and 2) an evaluation model for aesthetic consistency. To define a suitable design space for structural reinforcement and connector adaptation, we conducted a preliminary ideation session with designers. This process resulted in four update strategies, two of which involve inserting new structural members. We then parameterized these strategies—varying angles, positions, and dimensions—to generate a broad set of viable chair design alternatives. Furthermore, to evaluate these candidates, strength and fabrication cost can be estimated directly from geometry and material specifications. However, assessing aesthetic consistency is more complex. To address this, we collected human preferences through pairwise comparisons and modeled them using Crowd-BT, an approach for inferring a global ranking from noisy and potentially inconsistent human judgments [5]. The resulting aesthetic consistency model quantifies how well each design alternative preserves the base design’s visual impression.

The system was evaluated by running experiments examining the performance on four different wood species. We also tested different ranking policies—prioritizing structural strength, aesthetic consistency, or fabrication cost—demonstrating the outputs of different trade-offs. For instance, prioritizing structural integrity often resulted in reduced aesthetic consistency. We also performed multiple physical tests on different joint types, confirming that our structural simulation setup aligns reasonably well with reality. Finally, we fabricated a chair based on a system output.

In summary, we present UpJOINT, a design-assistance system that supports adapting a design to a variety of wood species, particularly in the context of locally sourced timber. Our contributions are:

- **A system for adapting a base chair design** made from wood components and 3D-printed connectors to different wood species, taking into account structural strength, aesthetic consistency, and fabrication cost.

- **A design space for reinforcement**, derived from a preliminary study that resulted in four update strategies—including the insertion of new structural members—based on which we produce a larger number of viable design alternatives.
- **An aesthetic consistency evaluation model**, based on crowd-sourced pairwise comparisons and inferred using the Crowd-BT algorithm, which enables quantitative evaluation of the preservation of the visual impression.

## 2 Related Works

### 2.1 Design and Analysis of Furniture

There is a large body of research focusing on computational assistance in the design of furniture and other small structures, many of which focuses on intuitive modeling interfaces and feedback or suggestions for improving physical validity and/or fabricability [3, 13, 32, 35, 36, 38, 39, 39]. The *FastForce* system introduces reinforcement strategies to improve the structural strength of laser-cut plate assemblies [3]. There is also a growing body of research focusing on parameterization of CAD models to enable intuitive parameter editing [12, 16] (to mention a few). Other work optimize furniture for specific properties, such as reconfigurability and interlocking [11, 33]. In contrast to the above work, our system includes a different design space of reinforcement strategies for chair frame assemblies specifically, and evaluates aesthetic consistency.

For aesthetic analysis, Liu et al. [24] proposed a method for evaluating style compatibility of 3D furniture models. Similar to our work, they built their system on crowd-sourced data. However, their focus is on selecting a set of furniture, while we focus on assessing the aesthetic consistency compared to a base design.

### 2.2 Computational Joinery

Advancements in 3D-printing, computer numerical control (CNC) milling, and laser cutting have driven a surge in research on joint modeling. The joint types of these systems can be roughly divided into two categories: 1) *integral joints*, where the geometry is part of the component itself [1, 2, 8, 14, 22, 23, 25, 27, 29, 34, 37, 39, 40], and 2) *external joints*, where a connector part joins multiple components [6, 7, 17–19, 26, 30]. This paper belongs to the second category of external joints, discussed in more detail below.

**2.2.1 External joints.** Magrisso et al. [26] introduced *Digital Joinery for Hybrid Carpentry*, a parametric system that generates 3D-printed joints to connect wooden beams at non-standard angles. They produce joints with Voronoi-based skeleton structures with parametric control of some appearance parameters, resulting in a novel furniture style. While they verify the strength of the joints, the joints are not optimized for structural performance.

Kovacs et al. [17, 18, 19] introduced *TrussFab*, *TrussFormer*, and *Trusscillator*—end-to-end systems that allow non-experts to design and fabricate large-scale structures from low cost materials. The material system consists of plastic bottles connected by 3D-printed joints forming triangular truss beams. They explored large-scale structures that can support human weight [19], and kinetic structures [17, 18]. While these systems visualize overall structural strength to verify safety, they do not implement optimization of structural performance or fabrication cost.

Chidambaram et al. [6] introduced *Shape Structuralizer*, an interactive system that translates surface models into structures made from rods and custom 3D-printed joints. Their system enables iterative generation and evaluation of structural designs through human-in-the-loop exploration of the design space. It verifies the strength of the overall structure, but does not analyze aesthetic consistency or fabrication costs.

Qiu et al. [30] proposed a system that automatically generates 3D-printed joints for wireframe structures, allowing for arbitrary-angle connections between dissimilar members while minimizing the number of unique joint types. While the system considers fabrication cost and shape preservation, it does not verify structural performance.

Colli et al. [7] proposed a topological optimization method for external joints that accounts for contact and friction. The resulting shapes exhibit improved structural performance, but do not account for changes in aesthetic consistency resulting from geometric deformation.

Finally, Nicolau et al. [28] presented a study comparing the structural strength of integral mortise-and-tenon joints with 3D-printed external joints similar to ours. Their study indicated that 3D-printed joints can be stronger than traditional ones, which motivated us to propose a system based on external joints.

### 3 Preliminary Study

To collect update strategies for structural reinforcement of a base chair, we conducted an ideation session. We aimed to explore a wide range of update ideas and classify them as general update strategies to be integrated into our system. For the session, we employed four university students (all male, 20–22 years old) with experience in designing and modeling furniture.

The session consisted of two phases. The first phase was a divergent ideation stage in which we asked participants to generate as many ideas as possible. In the second phase, we asked them to focus only on the joint parts, rather than proposing ideas that drastically changed the furniture design, such as adding or removing structural members. To facilitate the session, we provided reference images of chairs and physical wooden materials. We also asked them to focus on generalizable ideas. Participants searched for and discussed existing structural reinforcement approaches, and interacted with wooden materials prepared by the authors. Sticky notes were used to document the ideas, including text and sketches. Each phase took about 30 minutes, in total an hour.

After finishing the ideation phases, the participants grouped the collected ideas based on similarities, and then refined the groups so that each category was generalized and not overlapping each other. As a result, the participants conceived seven categories of design updates as in Fig. 2. These ideas included some judged to be infeasible, such as levitating the structure with magnets, changing the inner surface material to a honeycomb structure, and changing structures from beams to surfaces. Based on the grouped ideas shown in Fig. 2, we further abstracted and organized them into four categories of design updates— adding braces, adding bars, thickening members, and making the joints stronger (Fig. 3).

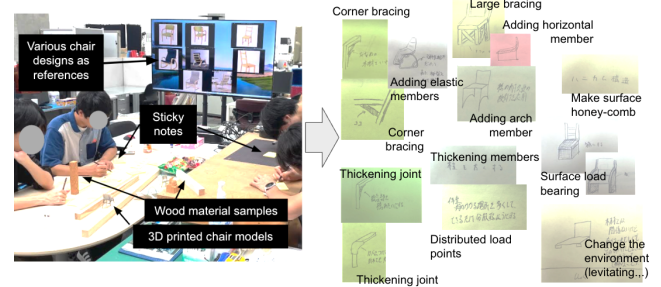


**Figure 2: The Ideation session and the generated design update ideas.**

## 4 System Overview

In this section, we clarify the inputs of the system (Section 4.1), how design candidates are created (Section 4.2), the different policies (Section 4.3) and finally the output of the system (Section 4.4). Fig. 1 shows an overview of the system.

### 4.1 Input

To begin, the system needs a base design with an assigned wood species, which is fixed in our current implementation. It is the reference for suggesting plausible design updates when the user specifies a different wood species. This assignment supplies the material parameters required for structural analysis. It also defines the baseline used to normalize structural scores. At run time, if a different species is selected, the solver substitutes the material parameters of the wooden members with those of the selected species and leaves the 3D-printed joints as defined. Thus, all evaluations use the selected species. The base assignment functions as a reference for normalization and reproducibility.

The base design comes with a 3D model consisting of wooden structural members and 3D-printed joints. The system also needs an analytical model consisting of lines and surfaces (see the right side of Fig. 11).

To calculate structural score, the user must specify a load value ( $kN$ ). The load value is a floating-point value and applied vertically to the seat during the simulation. The system has a fixed loading point on the base design.

Considering physical production of the suggested design, the user can set a range of fabrication cost such as [0 - 50]. The user can also specify a ranking policy, which is initially set to preserve aesthetic consistency. More details about the policies are provided in Section 4.3.

### 4.2 Design Variations

The system explores a design space defined by four update strategies from the preliminary study. Each strategy has one or two parameters, such as brace angle and length, bar height, member thickness, and joint shape. We manually assigned parameters for each strategy. By varying these parameters, we prepared 47 design variations as shown in the Appendix. We report the details of the preparation of the variations in Section 3.

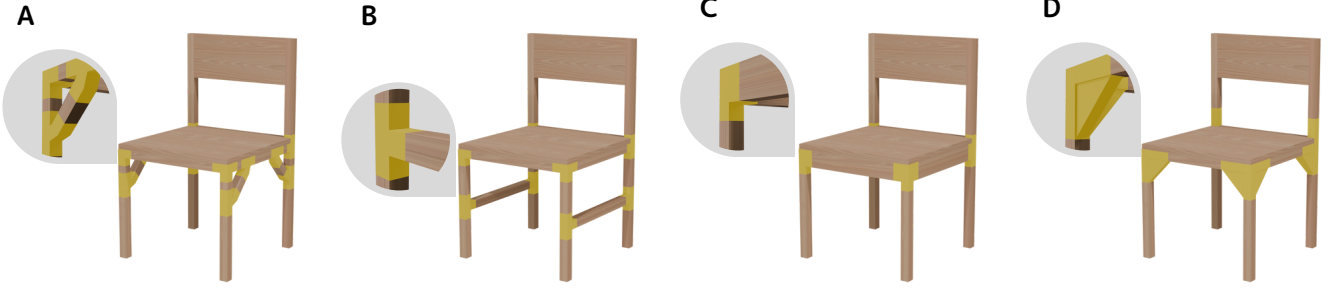


**Figure 3: Extracted design update strategies from the preliminary study: (A) diagonal braces; (B) horizontal bars; (C) thickening members; and (D) stronger joints.**

### 4.3 Policies and Scores

Although the policy of the system is primarily set to keep aesthetic consistency, we offer users to explore different “policies”, i.e., prioritizing aesthetic consistency or structurally soundness. In total, the system offers three different ranking policies: preserve the aesthetics of base design, prioritize bold updates, and minimize fabrication cost, denoted  $P_1$ ,  $P_2$ , and  $P_3$  respectively. To support this, a score calculation function with multiple criteria is introduced as in Eq. 1.

$$\text{Score} = w_{str} \cdot V_{str} + w_{aes} \cdot V_{aes} + w_{fab} \cdot V_{fab} \quad (\text{Eq. 1})$$

In Eq. 1, each design is evaluated by three criteria which are structural score, aesthetic consistency score, and fabrication cost, denoted  $V_{str}$ ,  $V_{aes}$ , and  $V_{fab}$  respectively. Multiplying a weight for each score (denoted as  $w_{str}$ ,  $w_{aes}$ , and  $w_{fab}$ ), we calculate a score for each design including the base design. We explain the details of score calculation in Section 5.1.

### 4.4 Output

The output screen displays the evaluation results based on the user inputs and the selected policy. Under  $P_1$  (the policy prioritizing aesthetic consistency), for example, the system proposes a 3D model that achieves the highest aesthetic consistency score while satisfying structural performance and fabrication cost. The 3D model allows users to visually check its whole design as well as 3D-printable joint parts.

For each output, the user can mark it as “Good” or “Not Good”. Selecting “Good”, the system exports the 3D-printable joint parts in STL or OBJ format. Selecting “Not Good” prompts the system to display the next-best update determined by Eq. 1. This iterative loop continues until a design that matches the user’s preferences is found.

## 5 System Implementation

In this section, we first explain the details of score calculations of the three criteria (structure strength, aesthetic consistency, and fabrication cost). For the calculation of aesthetic consistency, we conducted a crowd-sourced impression survey which is separately reported in (Section 5.2). Finally we report hardware and software of implementation (section 5.3).

### 5.1 Score Calculations

This section describes implementation details of calculation of the three scores (structural, aesthetic consistency, and fabrication).

**5.1.1 Structural Score.** Structural score  $V_{str}$  is calculated by the proportion of structural strength of the updated design based on the base design’s strength. The strength is calculated by Finite Element Analysis (FEA), more specifically the maximum value of the “Utilization” metric output by Karamba3D [15], which indicates the stress-to-capacity ratio under simulated load value.

After FEA is finished, the system computes the stress distribution throughout the model and extracts the maximum stress value based on the load input. This value is compared with the allowable stress provided by the selected wood species. If the maximum stress exceeds the allowable limit, the system judges it structurally unsafe and continues searching other updates; otherwise it returns “No update”.

In our evaluation, both wooden members and 3D-printed joints are checked, so the governing failure mode—including printed-joint failures observed in Fig. 8 controls feasibility. Allowable stresses for wood are taken from the user-selected species, and no additional safety factor is applied in the score (i.e.,  $\gamma = 1.0$ ). For ranking, we compare the “Utilization” metrics of the base and a candidate that are denoted as

$$V_{str} = \frac{U_{\text{cand}}}{U_{\text{base}}} \quad (\text{Eq. 2})$$

Here,  $U_{\text{base}}$  denotes the maximum utilization of the base design under the specified load case, and  $U_{\text{cand}}$  denotes the corresponding maximum utilization for a candidate update. By construction,  $V_{str} > 1$  indicates that the candidate performs better than the base,  $V_{str} = 1$  indicates the same as the base, and  $V_{str} < 1$  indicates worse performance.

**5.1.2 Fabrication Cost.** The system estimates the fabrication cost ( $V_{fab}$ ) ranges from -1.0 to 0.0, based on two components: wood cost and the material cost of 3D-printed parts. The wood and 3D-printing costs are calculated based on the number of additional wooden members and printed joints. Specifically, the costs of each additional wooden member and printed joint are set to 1.0 no matter what kind of printing materials and wood species. Furthermore, if a printed joint is larger than base design’s joint, its cost increases proportionally. When those parts were added, negative number of cost of the part is added to  $V_{fab}$ . The total fabrication cost becomes

a negative number. The design updates that exceed the specified max budget are excluded. To incorporate fabrication cost into the overall scoring function, we use the inverse of its absolute value.

$$V_{fab} = \frac{1}{x+\epsilon} - (\text{Eq. 3})$$

Where  $x$  denotes the predefined fabrication cost for each design update, and  $\epsilon$  is a small constant to prevent division by 0. In this formulation, lower-cost designs receive higher scores.

**5.1.3 Aesthetic Consistency Score and Crowd-BT Model.** The aesthetic consistency score ( $V_{aes}$ ) is calculated by Crowd-BT model [5], which is built upon an impression evaluation survey. Here we describe the model to calculate a ranking of pairwise evaluation of the survey. Crowd-BT model accounts for evaluator biases employed in crowd-sourcing on top of the Bradley-Terry (BT) model. This probabilistic model estimates rankings even when evaluator preferences are inconsistent or biased.

Using the Crowd-BT model, the resulting impression-impact vector  $s$ 's amplitude serves as the aesthetic-score term  $V_{aes}$  in Eq. 1 which are normalized to the range [0.0 - 1.0]. The vector  $s$  quantifies how much each design update deviates in impression from the base design. The vector  $s$  is calculated by solving the following optimization problem:

$$\underset{\eta, s}{\operatorname{Max}} L(\eta, s) + \lambda R(s) - (\text{Eq. 4})$$

$$\text{s.t. } 0 \leq \eta_k \leq 1, \forall k \in \{1, \dots, K\} - (\text{Eq. 5})$$

The functions  $L(\eta, s)$  and  $R(s)$  are defined as follows:

$$L(\eta, s) = \sum_{k=1}^K \sum_{(i,j) \in S_k} \log(\eta_k \frac{e^{s_i}}{e^{s_i} + e^{s_j}} + (1 - \eta_k) \frac{e^{s_j}}{e^{s_i} + e^{s_j}}) - (\text{Eq. 6})$$

$$R(s) = \sum_{i=1}^N (\log(\frac{e^{s_0}}{e^{s_0} + e^{s_i}}) + \log(\frac{e^{s_i}}{e^{s_0} + e^{s_i}})) - (\text{Eq. 7})$$

Here,  $\eta = (\eta_1, \dots, \eta_K)^T$  is evaluator reliabilities which is defined as a  $K$ -dimensional vector, where  $\eta_K \in [0, 1]$  represents a parameter indicating the extent to which evaluator  $a_K$ 's judgments align with those of an average evaluator. Higher values indicate stronger agreement with the average, while lower values indicate greater deviation. The model jointly estimates evaluator reliabilities  $\eta$  and  $s$  for each design option, improving ranking accuracy by solving optimization problem in Eq. 4 and Eq. 5.

## 5.2 Crowd-sourced Impression Survey

In this section describes the method to derive the aesthetic consistency ranking of 47 chair designs (see Fig. 15). We first report the impression evaluation survey conducted with crowd-sourced participants, and then describe the analysis of the results via CrowdBT model.

**5.2.1 Pairwise Impression Survey.** A straight-forward way to make a ranking is to ask all the participants to sort the 47 updates , however, it is a heavy task to remember all the candidates and switch back the order with trials and errors. Instead, we collected prepare chunks of pairwise comparisons and let participants focus on one comparison for each. For example in Fig 5,  $y_{14}$  and  $y_{22}$  are shown and a participant selects one of them that looks more different to the base design. This procedure requires only  $K + 1$  judgments to rank  $K$  pairs, whereas a full pairwise design requires  $2K$  judgments.

Which do you feel is different from the base design, chair A or chair B?



**Figure 4: Example task in the impression-evaluation survey.** A participant is asked to select A or B which is more different from the base design (on the far left).

The responses were stored on a per-participant, preserving each individual's response to every comparison. We then analyzed these response patterns to detect inconsistent or outlying behavior and estimated a reliability score for each participant. This reliability score was used as a weight when computing the aesthetic consistency ranking.

**5.2.2 Results of Crowd-sourced Survey.** The participants were recruited on a crowd-sourcing platform [21]. They were asked about prior experience with 3D CAD or furniture design. In total 376 people participated (227 male, 149 female; age 22–68, mean 44). 25 participants (18 male, 7 female) had 3D CAD experience and 15 participants (11 male, 4 female) had experience in furniture design.

Table 1 lists the five highest-ranked updates; all of them were judged to have only a minimal visual impact and therefore remain close to the base design (e.g., IDs  $y_{14}, y_{31}, y_{23}$ ). Conversely, Table 2 shows the five lowest-ranked updates, which evaluators perceived as markedly divergent from the baseline (e.g., IDs  $y_{22}, y_{30}, y_{13}$ ). The complete ranking of 47 update designs based on the  $P_1$  is provided in Fig. 10 in Appendix.

**Table 1: The top five impression impact ranking.**

Ranking	ID	$s_i$
1	$y_{14}$	1.00
2	$y_{31}$	$9.95 \times e^{-3}$
3	$y_{23}$	$9.81 \times e^{-3}$
4	$y_{21}$	$9.52 \times e^{-3}$
5	$y_{11}$	$9.50 \times e^{-3}$

Ranking	ID	$s_i$
47	$y_{22}$	0.00
46	$y_{30}$	$1.26 \times e^{-3}$
45	$y_{13}$	$4.29 \times e^{-3}$
44	$y_{17}$	$7.68 \times e^{-3}$
43	$y_{32}$	$7.74 \times e^{-3}$

## 5.3 Implementation Details

All processes were conducted on a computer with an Intel Core i7-7700HQ CPU and a GeForce GTX1050Ti graphic board. The system was developed using Rhinoceros 7 [31], along with its plugins Grasshopper, Karamba3D [15], and HumanUI [4]. These tools were integrated to enable seamless 3D modeling, structural analysis, and user interface creation.

The Crowd-BT model was implemented in R using the BradleyTerry2 package [9]. The Crowd-BT model in R are initialized by setting all  $\eta$  values to 1.0 and all  $s$  values to 0.0.



**Figure 5: The best ( $y_{14}$ ) and the worst ( $y_{22}$ ) of the ranking comparing with the base design.**

The connection between wooden members and 3D-printed parts is a mortise and tenon joint whose section is a square shape (Figure 6). The edge of wooden members are offset inward, and 3D-printed parts are engraved as it has inverted shape.

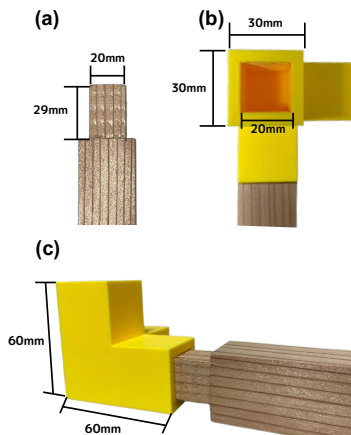


**Figure 6: A close-up of a joint-member connection. (a) Tenon part of the wooden member, inset by 5 mm on each side from the original 30 mm  $\times$  30 mm section. (b) Mortise on the 3D-printed joint, matching the tenon dimensions. (c) Assembled state showing the mortise and tenon joint with a 60 mm  $\times$  60 mm 3D-printed part.**

For Mechanical testing, joints were fabricated on a Flashforge Adventurer 5M [10] (0.40 mm nozzle, PLA, layer height = 0.20 mm). The prototype's joints were fabricated on a Zortrax M200 Plus [41] (0.40 mm nozzle, PLA, layer height = 0.20 mm). The wooden members used for the assembly measured 30 mm in width, 30 mm height, and 300 mm length.

## 6 Evaluation

We evaluated the system under the given input conditions from  $C_1$  to  $C_4$  in Table 4. We test these conditions with the three design policies ( $P_1$ ,  $P_2$ , and  $P_3$ ), and analyze how much improvement each test achieved the results.

### 6.1 Conditions

The system was tested under specific conditions (Table 4), and the design updates based on those conditions were analyzed. The parameters in the given conditions are wood species, load, and fabrication costs. In  $C_1$  and  $C_2$ , we examined whether the system could produce appropriate outputs under different loading conditions. In  $C_3$ , we tested whether the system could still generate valid designs when a high load was applied to a weaker wood species.  $C_4$  was designed to verify if “No update” are suggested by the system with conditions that do not require extra reinforcement.

Three preference policies multiplied by four conditions, a total of 12 validations were tested. We used the following weights for each policy as in Table 3.

**Table 3: Weight values for policies**

Policies	$w_{str}$	$w_{aes}$	$w_{fab}$
$P_1$	1.0	2.0	1.0
$P_2$	1.0	-2.0	1.0
$P_3$	1.0	1.0	2.0

**Table 4: The conditions for validation of the system.**

ID	Wood types		
	[Young's modulus( $kN/cm^2$ )]	Load value [kg]	Max fab cost
$C_1$	Ceder [750]	100	30
$C_2$	Ceder [750]	110	10
$C_3$	White birch [830]	150	15
$C_4$	Oak [1200]	120	8

**Table 5: Results of structural score.**

ID	$P_1$	$P_2$	$P_3$
$C_1$	0.53	0.97	0.23
$C_2$	0.81	0.86	0.64
$C_3$	0.76	0.89	0.87
$C_4$	—	—	—

**Table 6: Results of fabrication cost.**

ID	$P_1$	$P_2$	$P_3$
$C_1$	-0.81	-0.70	-0.23
$C_2$	-0.54	-0.70	-0.36
$C_3$	-0.81	-0.70	-0.36
$C_4$	—	—	—

**Table 7: Results of aesthetics consistency scores.**

ID	$P_1$	$P_2$	$P_3$
$C_1$	0.98	0.00	0.94
$C_2$	0.63	0.00	0.53
$C_3$	0.98	0.00	0.94
$C_4$	1.00	1.00	1.00

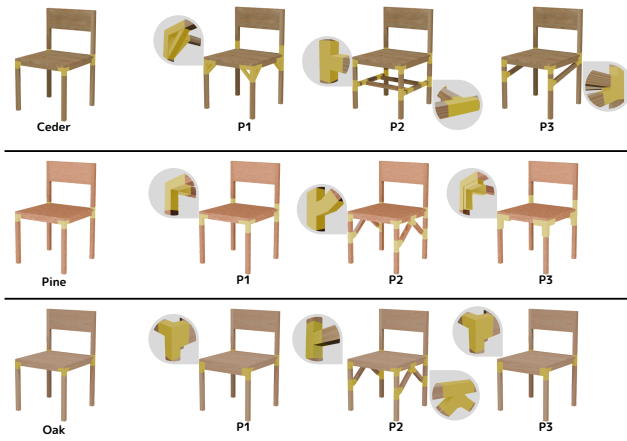


**Figure 7: Examples of chair design updates under the three policies (P1, P2, and P3).**

## 6.2 Results

As in Table 5 presents the results of the structural score. For details on how the structural score is calculated, please refer to Section 5.1.1. Notably, the prioritize bold updates policy (*P2*) yielded the greatest reduction, contributing to structural strength. In contrast, the preserve aesthetics and minimize cost policies (*P1* and *P3* respectively) also enhanced structural strength but showed more limited improvements due to smaller design adjustments. Over prolonged use, these policies raise concerns about structural strength compared to *P2*. As in Table 7, aesthetic scores were highest under *P1*, reaching 0.98 in C1, which closely mirrored the base design. In contrast, *P2* recorded score of zero, indicating they completely failed to preserve the base design. While the minimize fabrication cost policy (*P3*) sometimes maintained moderate aesthetic levels, its scores remained lower than those achieved by *P1*.

## 6.3 Mechanical Testing

This study employed a destructive load test to evaluate the mechanical performance of the proposed joint. The test was performed on both the base design's joint and the updated joint, with three identical specimens prepared for each design to enable statistical comparison. All tests were performed on an IMADA motorized test stand (MX-500 N) equipped with an IMADA digital force gauge(DST-1000 N, measurement range 0–1000 N).

Each specimen consisted of a parts of the chair leg fitted with the 3D-printed joint and measured 300 mm in height and 270 mm in width (see Fig. 12). A wooden support block (height: 105 mm, width: 90 mm) was screwed to a plywood base to clamp the specimen (see Fig. 12—position 1). A single point compressive load was applied vertically from above and positioned 160 mm to the left of the joint (see Fig. 12—position 2). The load was increased continuously from 0 N to 500 N.

During the destructive test, load was applied continuously until the specimen failed. All load data were recorded in CSV format, and the failure process, including fracture of the 3D-printed joint, was documented with video and photographs.

**Table 8: Comparison of fracture loads between physical tests and simulations for the two joint designs. (A) Base design's joint; (B) Updated joint. The physical-test values represent the median fracture load obtained from three specimens.**

Joint	Physical test [N]	Simulation [N]
A	86	93
B	126	130

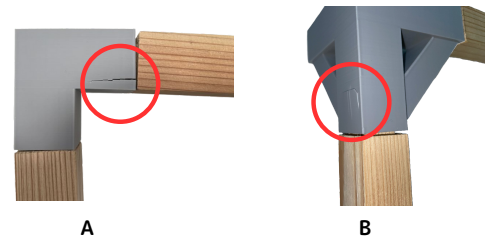


**Figure 8: Connector failure; (A) Base design's joint; (B) Updated joint.**

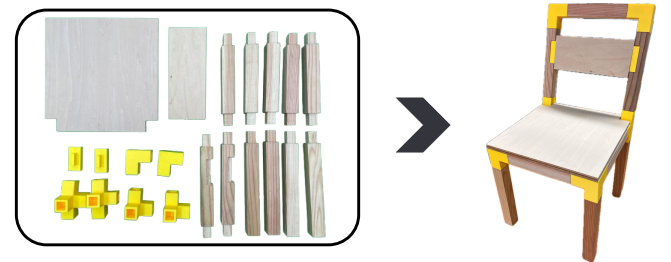


**Figure 9: Prototype produced from the system output. (Left) 3D-printed joints, cedar beams, and plywood parts laid out before assembly. (Right) Completed chair assembled.**

The fractures were observed after the destructive load test is presented in Fig. 8. The left image of Fig. 8 shows the base design's joint, where the seat-rail mortise fractured along the 3D-printing layer direction. The right image of Fig. 8 shows the updated joint, where the leg-member mortise failed along the same lamination direction. In both cases, the experimentally measured failure load was lower than the load associated with the maximum stress predicted by the FEA.

## 6.4 Physical Prototype

We fabricated a prototype using cedar and PLA joints. The left image of Fig. 9 shows all components prior to assembly: 3D-printed joints (yellow), milled cedar beams, and plywood seat/back panels. The right image of Fig. 9 shows presents the assembled chair. No additional fasteners were required; press-fit tolerance was set to 0.15 mm.

## 7 Discussion

In this section, we discuss the update tendencies, score variations, and trade-off observed under the three policies, based on the evaluation results.

### 7.1 Structural Score

Table 5 confirmed that structural performance improved after design updates under all the three policies. In particular, *P2* showed significant improvements in structural scores due to the bold global design update. Meanwhile, *P1* achieved a balance between aesthetic consistency and structural strength, maintaining a design close to the base design while improving capability. Under *P3*, design update aimed at cost reduction also achieved moderate improvements in capability. These results indicate that the proposal policies adequately satisfied structural requirements.

### 7.2 Aesthetic Consistency

Table 7 In particular, *P1* achieved the highest scores, demonstrating a high degree of similarity to the base design. This success likely stems from adding structural elements and dimensional changes without disrupting visual and perceptual consistency. In contrast, *P2* showed a decrease in aesthetic consistency scores due to extensive design update. Under this policy, significant changes in the placement of joints and reinforcement materials led to noticeable deviations from the base design. Similarly, *P3* showed a slight decline in aesthetic consistency scores due to prioritizing cost reduction. These findings suggest a trade-off between aesthetic consistency and metrics like structural strength and fabrication costs.

This case study with the simple chair design was limited, but design updates may different impact user impressions in more complex or decorative designs. For example, in chairs with textured surfaces or decorative designs, changes to reinforcement materials or joint shapes could more noticeable impact on overall aesthetics. Additionally, in chair designs that already include reinforcement structures such as diagonal braces or horizontal bars, similar design updates may help preserve aesthetics more effectively. As a results, it is possible that the impact on impressions revealed in this study may exhibit different tendencies.

## 8 Conclusion

As a summary, this paper presented a design-assist system to support the use of diverse wood species in furniture making. To address the challenges of varying physical properties across wood species, we use 3D-printed joints that allow for flexible design updates without needing to remake wood machining setups—such as changing jigs or tooling—by keeping the wooden parts consistent and adapting only the connector designs. While prior work has explored 3D-printed joints customizability and strength, we highlight their untapped potential in enabling flexible sourcing of wood. Finally, our impression evaluation study, analyzed using the Crowd-BT model, adds an important dimension to the system by providing objective, data-driven rankings of aesthetic similarity to the base model.

One of the biggest limitation of our work is that the calculation of aesthetic similarity is applicable only for the chair model appeared

in Fig. 1 and other figures. Generalizing the approach to support a broader range of furniture types and structural configurations—such as tables, shelves, and beds—would require two key extensions: (1) expanding the library of joint types and reinforcements to support a more diverse set of connections, and (2) collecting additional crowd-sourced data to enable ranking of types of structures. In addition, the current optimization strategy relies on exhaustive search over a discrete design space. It would be valuable to explore more advanced optimization methods, incorporating continuous design parameters and employing a more advanced optimization framework for more efficient exploration of the design space and greater flexibility in generating high-performing solutions, especially if the complexity of the problem increases—with more connection types and structural variations. Furthermore, future systems could incorporate an interactive feedback loop in which design suggestions are informed by accumulated user feedback, enabling automation of personalized design updates.

## Acknowledgments

We would like thank the crowd workers participated in our study. This work was inspired by the visits in several saw mills and furniture manufactures in Hokkaido, Japan. This project was supported by JSPS KAKENHI grant number 50728087, Future University Hakodate Competitive Internal Grant (Priority Area), and art-ai-fact from Aalto University.

## References

- Muhammad Abdullah, Laurenz Seidel, Ben Wernicke, Mehdi Gouasmi, Anton Hackl, Thomas Kern, Conrad Lempert, Clara Lempert, David Bizer, Wieland Storch, Chiao Fang, and Patrick Baudisch. 2024. PopCore: Personal Fabrication of 3D Foamcore Models for Professional High-Quality Applications in Design and Architecture. In *Proceedings of the 9th ACM Symposium on Computational Fabrication* (Aarhus, Denmark) (SCF '24). Association for Computing Machinery, New York, NY, USA, Article 6, 14 pages. doi:10.1145/3639473.3665787
- Muhammad Abdullah, Romeo Sommerfeld, Bjarne Sievers, Leonard Geier, Jonas Noack, Marcus Ding, Christoph Thieme, Laurenz Seidel, Lukas Fritzsche, Erik Langenhan, Oliver Adameck, Moritz Dzingel, Thomas Kern, Martin Taraz, Conrad Lempert, Shohei Katakura, Hany Mohsen Elhassany, Thijs Roumen, and Patrick Baudisch. 2022. HingeCore: Laser-Cut Foamcore for Fast Assembly. In *Proceedings of the 35th Annual ACM Symposium on User Interface Software and Technology* (Bend, OR, USA) (UIST '22). Association for Computing Machinery, New York, NY, USA, Article 10, 13 pages. doi:10.1145/3526113.3545618
- Muhammad Abdullah, Martin Taraz, Yannis Kommana, Shohei Katakura, Robert Kovacs, Jotaro Shigeyama, Thijs Roumen, and Patrick Baudisch. 2021. FastForce: Real-Time Reinforcement of Laser-Cut Structures. In *Proceedings of the 2021 CHI Conference on Human Factors in Computing Systems* (Yokohama, Japan) (CHI '21). Association for Computing Machinery, New York, NY, USA, Article 673, 12 pages. doi:10.1145/3411764.3445466
- Andrew Heumann. [n. d.]. Human UI for Grasshopper. <https://www.food4rhino.com/en/app/human-ui>. Accessed: July 17, 2025.
- Xi Chen, Paul N. Bennett, Kevyn Collins-Thompson, and Eric Horvitz. 2013. Pairwise Ranking Aggregation in a Crowdsourced Setting. In *Proceedings of the Sixth ACM International Conference on Web Search and Data Mining* (WSDM '13). ACM, 193–202.
- Subramanian Chidambaram, Yunbo Zhang, Venkatraghavan Sundararajan, Niklas Elmquist, and Karthik Ramani. 2019. Shape Structuralizer: Design, Fabrication, and User-Driven Iterative Refinement of 3D Mesh Models. In *Proceedings of the 2019 CHI Conference on Human Factors in Computing Systems*. ACM, Glasgow, Scotland, UK, 1–12. doi:10.1145/3290605.3300893
- Tozoni Davi Colli, Yunfan Zhou, and Denis Zorin. 2021. Optimizing Contact-Based Assemblies. *ACM Transactions on Graphics* 40, 6 (Dec 2021), 269:1–269:19.
- Mustafa Doga Dogan, Vivian Hsinyueh Chan, Richard Qi, Grace Tang, Thijs Roumen, and Stefanie Mueller. 2023. StructCode: Leveraging Fabrication Artifacts to Store Data in Laser-Cut Objects. In *Proceedings of the 8th ACM Symposium on Computational Fabrication* (New York City, NY, USA) (SCF '23). Association for Computing Machinery, New York, NY, USA, Article 6, 13 pages. doi:10.1145/3623263.3623353

- David Firth and Heather Turner. [n. d.]. BradleyTerry2: Bradley-Terry Models. <https://cran.r-project.org/web/packages/BradleyTerry2/index.html>. Accessed: July 17, 2025.
- FlashForge Japan. [n. d.]. Adventurer 5M. <https://flashforge.jp/product/adventurer5m/>. Accessed: July 17, 2025.
- Chi-Wing Fu, Peng Song, Xiaoqi Yan, Lee Wei Yang, Pradeep Kumar Jayaraman, and Daniel Cohen-Or. 2015. Computational interlocking furniture assembly. *ACM Trans. Graph.* 34, 4, Article 91 (July 2015), 11 pages. doi:10.1145/2766892
- Aditya Ganeshan, Ryan Huang, Xianghao Xu, R. Kenny Jones, and Daniel Ritchie. 2024. ParSEL: Parameterized Shape Editing with Language. *ACM Trans. Graph.* 43, 6, Article 197 (Nov. 2024), 14 pages. doi:10.1145/3687922
- Ramya Iyer, Mustafa Dogan, Maria Larsson, and Takeo Igarashi. 2025. XR-penter: Material-Aware and In Situ Design of Scrap Wood Assemblies. In *Proceedings of the 2025 CHI Conference on Human Factors in Computing Systems (CHI '25)*. Association for Computing Machinery, New York, NY, USA, Article 689, 16 pages. doi:10.1145/3706598.3713331
- Kenji Kanasaki and Hiroya Tanaka. 2013. Traditional Wood Joint System in Digital Fabrication. *Computation and Performance - Proceedings of the 31st eCAADe Conference 2013* (2013), 711–717. <http://resolver.tudelft.nl/uuid:d36152ad-7fcf-44b6-bdfe-654f159a3e65>
- Karamba3D Team. [n. d.]. Karamba3D: Parametric Structural Engineering. <https://karamba3d.com/>. Accessed: July 17, 2025.
- Milin Kodnongbua, Benjamin Jones, Maaz Bin Safeer Ahmad, Vladimir Kim, and Adriana Schulz. 2023. ReparamCAD: Zero-shot CAD Re-Parameterization for Interactive Manipulation. In *SIGGRAPH Asia 2023 Conference Papers* (Sydney, NSW, Australia) (SA '23). Association for Computing Machinery, New York, NY, USA, Article 69, 12 pages. doi:10.1145/3610548.3618219
- Robert Kovacs, Alexandra Ion, Pedro Lopes, Tim Oesterreich, Johannes Filter, Philipp Otto, Tobias Arndt, Nico Ring, Melvin Witte, Anton Syntysia, and Patrick Baudisch. 2018. TrussFormer: 3D Printing Large Kinetic Structures. In *Proceedings of the 31st Annual ACM Symposium on User Interface Software and Technology* (Berlin, Germany) (UIST '18). Association for Computing Machinery, New York, NY, USA, 113–125. doi:10.1145/3242587.3242607
- Robert Kovacs, Lukas Rambold, Lukas Fritzsche, Dominik Meier, Jotaro Shigeyama, Shohei Katakura, Ran Zhang, and Patrick Baudisch. 2021. Trusscillator: a System for Fabricating Human-Scale Human-Powered Oscillating Devices. In *The 34th Annual ACM Symposium on User Interface Software and Technology (Virtual Event, USA) (UIST '21)*. Association for Computing Machinery, New York, NY, USA, 1074–1088. doi:10.1145/3472749.3474807
- Robert Kovacs, Anna Seufert, Ludwig Wall, Hsiang-Ting Chen, Florian Meinel, Willi Müller, Sijing You, Maximilian Brehm, Jonathan Striebel, Yannis Kommana, Alexander Popiak, Thomas Bläsius, and Patrick Baudisch. 2017. TrussFab: Fabricating Sturdy Large-Scale Structures on Desktop 3D Printers. In *Proceedings of the 2017 CHI Conference on Human Factors in Computing Systems (CHI '17)*. ACM, Denver, CO, USA, 2606–2616. doi:10.1145/3025453.3026016
- Yuki Koyama, Shinjiro Sueda, Emma Steinhardt, Takeo Igarashi, Ariel Shamir, and Wojciech Matusik. 2015. AutoConnect: Computational Design of 3D-Printable Connectors. *ACM Transactions on Graphics* 34, 6 (November 2015), 231:1–231:11. doi:10.1145/2816795.2818060
- Lancers Inc. [n. d.]. Lancers: A Platform for Freelancers and Clients. <https://www.lancers.jp>. Accessed: January 23, 2025.
- M. Larsson, H. Yoshida, N. Umetani, and T. Igarashi. 2020. Tsugite: Interactive Design and Fabrication of Wood Joints. In *Proceedings of the 33rd Annual ACM Symposium on User Interface Software and Technology (UIST '20)*. ACM, 529–540.
- Danny Leen, Tom Veuskens, Kris Luyten, and Raf Ramakers. 2019. JigFab: Computational Fabrication of Constraints to Facilitate Woodworking with Power Tools. In *Proceedings of the 2019 CHI Conference on Human Factors in Computing Systems* (Glasgow, Scotland UK) (CHI '19). ACM, New York, NY, USA, Article 156, 12 pages. doi:10.1145/3290605.3300386
- Tianqiang Liu, Aaron Hertzmann, Wilmot Li, and Thomas Funkhouser. 2015. Style compatibility for 3D furniture models. *ACM Trans. Graph.* 34, 4, Article 85 (July 2015), 9 pages. doi:10.1145/2766898
- Linjie Luo, Ilya Baran, Szymon Rusinkiewicz, and Wojciech Matusik. 2012. Chopper: partitioning models into 3D-printable parts. *ACM Trans. Graph.* 31, 6, Article 129 (Nov. 2012), 9 pages. doi:10.1145/2366145.2366148
- S. Magrissio, M. Mizrahi, and A. Zoran. 2018. Digital Joinery for Hybrid Carpentry. In *Proceedings of the 2018 CHI Conference on Human Factors in Computing Systems (CHI '18)*. ACM, 1–12.
- Atsushi Maruyama, Maria Larsson, I-Chao Shen, and Takeo Igarashi. 2024. Designing Reconfigurable Joints. In *SIGGRAPH Asia 2024 Technical Communications (SA '24)*. Association for Computing Machinery, New York, NY, USA, Article 34, 4 pages. doi:10.1145/3681758.3698006
- Antoni Nicolau, Marius Nicolae Baba, Camelia Cerbu, Cătălin Cioacă, Luminița-Maria Brenci, and Camelia Coseoreanu. 2025. Evaluation of 3D-Printed Connectors in Chair Construction: A Comparative Study with Traditional Mortise-and-Tenon Joints. *Materials* 18, 1 (2025). doi:10.3390/ma18010201
- Keunwoo Park, Conrad Lempert, Muhammad Abdullah, Shohei Katakura, Jotaro Shigeyama, Thijs Roumen, and Patrick Baudisch. 2022. FoolProofJoint: Reducing Assembly Errors of Laser Cut 3D Models by Means of Custom Joint Patterns. In *Proceedings of the 2022 CHI Conference on Human Factors in Computing Systems* (New Orleans, LA, USA) (CHI '22). Association for Computing Machinery, New York, NY, USA, Article 271, 12 pages. doi:10.1145/3491102.3501919
- Pengyu Qiu, Rulin Chen, Peng Song, , and Ying He. 2025. Modeling Wireframe Meshes with Discrete Equivalence Classes. *IEEE Transactions on Visualization and Computer Graphics* (2025).
- Robert McNeel & Associates. [n. d.]. Rhinoceros 3D. <https://www.rhino3d.com/jp/>. Accessed: July 17, 2025.
- Adriana Schulz, Ariel Shamir, David I. W. Levin, Pitchaya Sitthi-amorn, and Wojciech Matusik. 2014. Design and fabrication by example. *ACM Trans. Graph.* 33, 4, Article 62 (July 2014), 11 pages. doi:10.1145/2601097.2601127
- Peng Song\*, Chi-Wing Fu\*, Yueming Jin, Hongfei Xu, Ligang Liu, Pheng-Ann Heng, and Daniel Cohen-Or. 2017. Reconfigurable Interlocking Furniture. *ACM Transactions on Graphics (SIGGRAPH Asia)* 36, 6 (2017), 174:1–17:14. \* joint first author.
- Rundong Tian, Sarah Sterman, Ethan Chiou, Jeremy Warner, and Eric Paulos. 2018. MatchSticks: Woodworking through Improvisational Digital Fabrication. In *Proceedings of the 2018 CHI Conference on Human Factors in Computing Systems* (Montreal QC, Canada) (CHI '18). Association for Computing Machinery, New York, NY, USA, 1–12. doi:10.1145/3173574.3173723
- N. Umentani, T. Igarashi, and N. J. Mitra. 2015. Guided Exploration of Physically Valid Shapes for Furniture Design. *Commun. ACM* 58, 9 (2015), 116–122.
- Ziqi Wang, Peng Song, and Mark Pauly. 2018. DESIA: a general framework for designing interlocking assemblies. *ACM Trans. Graph.* 37, 6, Article 191 (Dec. 2018), 14 pages. doi:10.1145/3272127.3275034
- Ziqi Wang, Peng Song, and Mark Pauly. 2021. MOCCA: modeling and optimizing cone-joints for complex assemblies. *ACM Trans. Graph.* 40, 4, Article 181 (July 2021), 14 pages. doi:10.1145/3450626.3459680
- Chenming Wu, Haisen Zhao, Chandrakana Nandi, Jeffrey I. Lipton, Zachary Tatlock, and Adriana Schulz. 2019. Carpentry compiler. *ACM Trans. Graph.* 38, 6, Article 195 (Nov. 2019), 14 pages. doi:10.1145/3355089.3356518
- J. Yao, D. M. Kaufman, Y. Gingold, and M. Agrawala. 2017. Interactive Design and Stability Analysis of Decorative Joinery for Furniture. *ACM Transactions on Graphics (TOG)* 36, 2 (2017), 20:1–20:16.
- Clement Zheng, Ellen Yi-Luen Do, and Jim Budd. 2017. Joinery: Parametric Joint Generation for Laser Cut Assemblies. In *Proceedings of the 2017 ACM SIGCHI Conference on Creativity and Cognition* (Singapore, Singapore) (C&C '17). Association for Computing Machinery, New York, NY, USA, 63–74. doi:10.1145/3059454.3059459
- Zortrax. [n. d.]. Zortrax M200 Plus. <https://zortrax.com/3d-printers/m200-plus/>. Accessed: July 17, 2025.

## A Appendix

### A.1 Design Candidates

Fig. 15 shows the full set of design candidates—discrete outputs of the parameterized designs based on the four design update strategies (refer to Fig. 3), which were determined in the preliminary study (refer to Fig. 3).

Fig. 14 shows the adaptation of the design update strategies (refer to Fig. 3), which were determined in the preliminary study (refer to Fig. 3)—were adapted to the stool model.

### A.2 The Results of Crowd-BT Detail

Fig. 10 shows the ranking results of all 47 design candidates estimated by the Crowd-BT model. These rankings are based on pairwise comparison data collected from participants during the impression evaluation and reflect the inferred preference tendency for each candidate. The results complement Table 1 and Table 2 presented in Section 5.2.3. This ranking corresponds to the P1 (the policy prioritizing aesthetic consistency).

### A.3 Details of the Simulation and Mechanical Tests

Finite Element Analysis (FEA) needs the following information: wood species, models of the base design (a 3D mesh model and an analytical model), and loading conditions (with a load value and its direction, and a loading point). When a wood species is selected, the system retrieves its mechanical specifications such as Young's modulus, shear modulus, and yield stresses for different directions ( $kN/cm^2$ ), and specific weight ( $kN/cm^3$ ). Fig. 11 shows the mesh and analysis models—(A) the design-interaction mesh and (B) the structural analysis model composed of beam and shell elements.

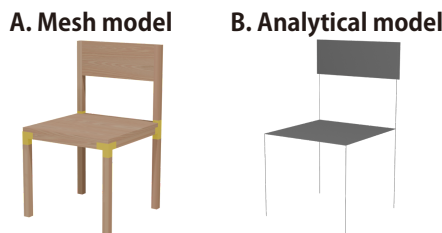


**Figure 11: Comparison between (A) the mesh model used for design interaction and (B) the analytical model used for structural simulation. The analytical model consists of beam and shell elements.**

Fig. 12 shows the experimental setup for the mechanical test. (A) represents the setup for the base design's joint, and (B) represents the setup for the updated joint. The loading position and overall dimensions were kept identical for both conditions. Each specimen, composed of a portion of a chair leg and a 3D-printed joint, was fixed to a plywood base using a wooden support block (position 1 in Fig. 12 A). A single-point load was applied vertically from above, 160 mm away from the joint (position 2 in Fig. 12 A), increasing continuously from 0 N to 500 N. Force data were recorded at a rate of 10 frames per second.

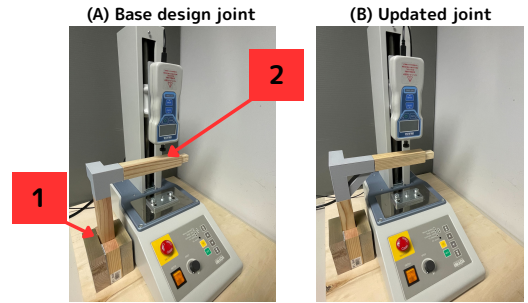
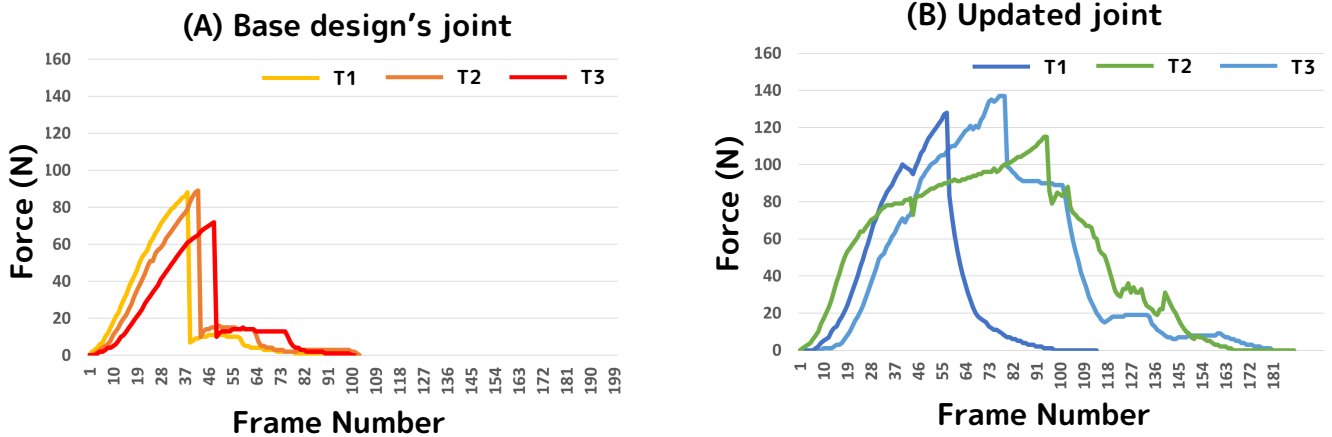


**Figure 12: Chairs preparation on the test; (A) Base design's joint; (B) Updated joint.**

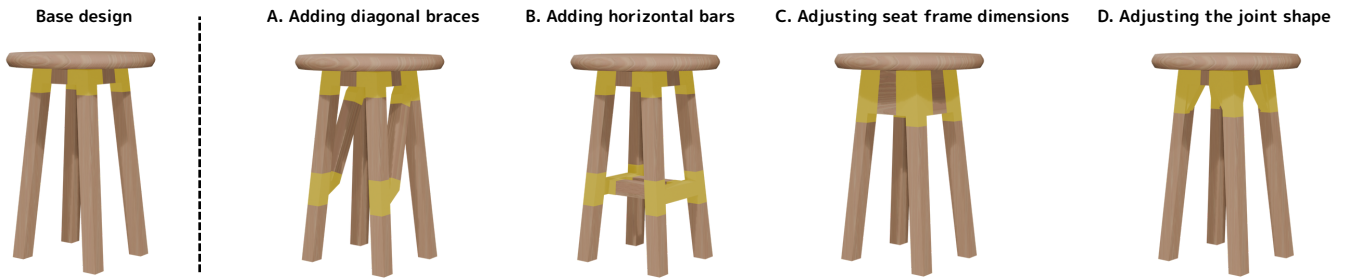
In Fig. 13 shows the force–frame-number curves obtained from the destructive tests. (A) shows the results of three trials for the base design's joint, while (B) shows those for the updated joint. The tests were conducted under identical loading conditions to compare their structural strength.

Ranking	ID	$s_i$	Ranking	ID	$s_i$	Ranking	ID	$s_i$	Ranking	ID	$s_i$
1		1.0000	11		0.8265	21		0.5095	31		0.4297
2		0.9955	12		0.6632	22		0.5053	32		0.3969
3		0.9812	13		0.6284	23		0.4923	33		0.3683
4		0.9527	14		0.6057	24		0.4869	34		0.3640
5		0.9502	15		0.5628	25		0.4815	35		0.3136
6		0.9469	16		0.5486	26		0.4721	36		0.2513
7		0.9243	17		0.5420	27		0.4577	37		0.1760
8		0.8966	18		0.5275	28		0.4559	38		0.1310
9		0.8962	19		0.5225	29		0.4523	39		0.1099
10		0.8313	20		0.5113	30		0.4399	40		0.1029
											0.1018
											0.0860
											0.0774
											0.0768
											0.0429
											0.0126
											0.0000

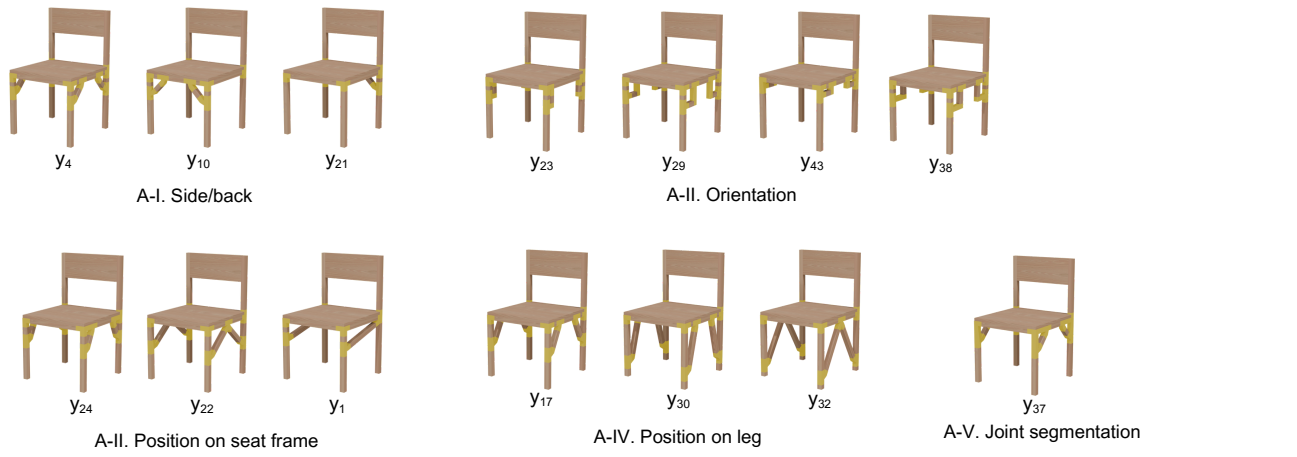
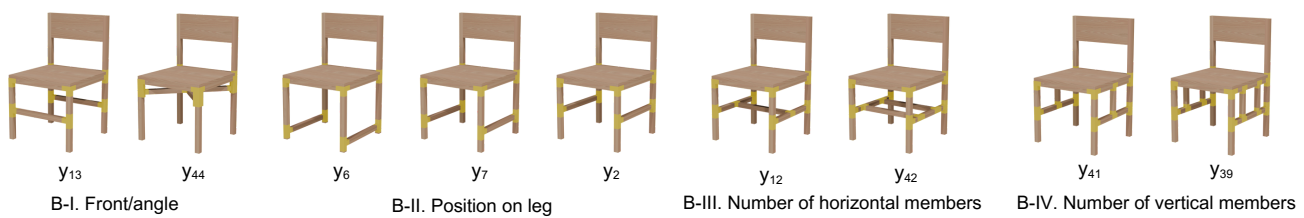
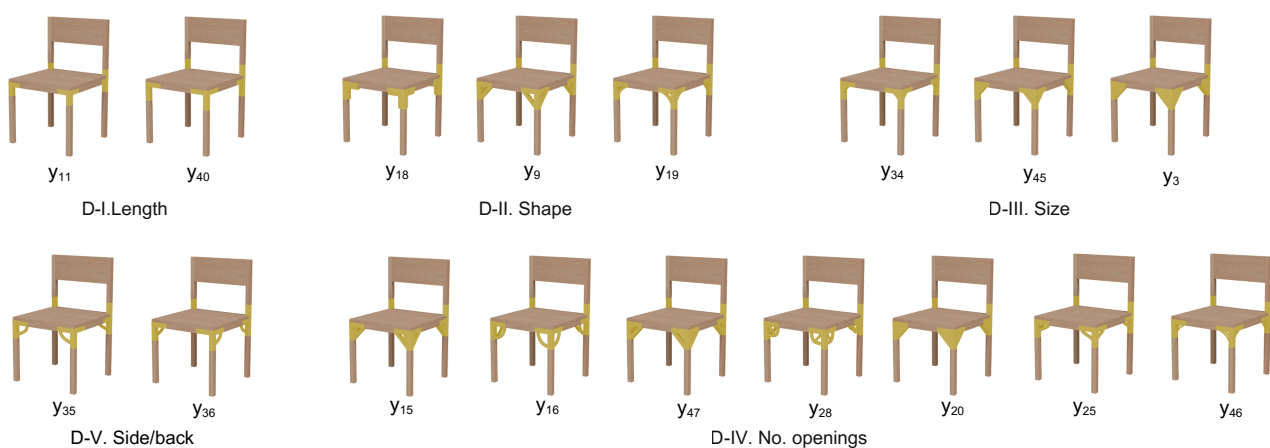
Figure 10: Complete ranking results estimated by the Crowd-BT model under the  $P_1$  (the policy prioritizing aesthetic consistency).



**Figure 13:** Force–frame-number curves obtained from the destructive tests. A: three trials for the base-design joint. B: three trials for the updated joint



**Figure 14:** Extracted design update strategies applied to the stool version: (A) diagonal braces, (B) horizontal bars, (C) thickening members, and (D) stronger joints.

**A. Adding diagonal braces****B. Adding horizontal bars****C. Adjusting seat frame dimensions****D. Adjusting the joint shape**

**Figure 15: Parameterized design variations used in the impression evaluation survey. Each column visualizes the chair after systematically varying a single parameter within one of the four update strategies presented in Figure 3.**